Published in final edited form as:
Psychoneuroendocrinology. 2014 July ; 45: 128–141. doi:10.1016/j.psyneuen.2014.03.023.

The neuroanatomical distribution of oxytocin receptor binding and mRNA in the male rhesus macaque (*Macaca mulatta*)

Sara M. Freeman, Ph.D[*], **Kiyoshi Inoue, Ph.D**, **Aaron L. Smith, Ph.D**, **Mark M. Goodman, Ph.D**, and **Larry J. Young, Ph.D**

Center for Translational Social Neuroscience; Silvio O. Conte Center for Oxytocin and Social Cognition; Department of Psychiatry and Behavioral Sciences; Yerkes National Primate Research Center; Emory University, Atlanta, GA 30029, USA

Abstract

The rhesus macaque (*Macaca mulatta*) is an important primate model for social cognition, and recent studies have begun to explore the impact of oxytocin on social cognition and behavior. Macaques have great potential for elucidating the neural mechanisms by which oxytocin modulates social cognition, which has implications for oxytocin-based pharmacotherapies for psychiatric disorders such as autism and schizophrenia. Previous attempts to localize oxytocin receptors (OXTR) in the rhesus macaque brain have failed due to reduced selectivity of radioligands, which in primates bind to both OXTR and the structurally similar vasopressin 1a receptor (AVPR1A). We have developed a pharmacologically-informed competitive binding autoradiography protocol that selectively reveals OXTR and AVPR1A binding sites in primate brain sections. Using this protocol, we describe the neuroanatomical distribution of OXTR in the macaque. Finally, we use *in situ* hybridization to localize OXTR mRNA. Our results demonstrate that OXTR expression in the macaque brain is much more restricted than AVPR1A. OXTR is largely limited to the nucleus basalis of Meynert, pedunculopontine tegmental nucleus, the superficial gray layer of the superior colliculus, the trapezoid body, and the ventromedial hypothalamus. These regions are involved in a variety of functions relevant to social cognition, including modulating visual attention, processing auditory and multimodal sensory stimuli, and controlling orienting responses to visual stimuli. These results provide insights into the neural mechanisms by which oxytocin modulates social cognition and behavior in this species, which, like humans, uses vision and audition as the primary modalities for social communication.

[*]Corresponding Author: Sara M. Freeman, Ph.D. California National Primate Research Center- BMB University of California, Davis One Shields Ave. Davis, CA 95616 smfreem@ucdavis.edu Telephone: 530.752.1506 Fax: 530.754.8166.

CONTRIBUTORS

SMF and LJY designed the study. SMF performed all experiments except the in situ hybridization, which was performed by KI. ALS designed and synthesized the novel antagonist used in the study under advisement of MMG. LJY funded the research. SMF performed all analysis and wrote the first draft of the manuscript. All authors have contributed to and have approved the final manuscript.

CONFLICT OF INTEREST

The authors declare no conflicts of interest.

Keywords

oxytocin receptor; neuropeptide; neuroanatomy; nonhuman primate; autism

INTRODUCTION

Oxytocin (OT) and vasopressin (AVP) are structurally related peptides that modulate a range of complex social behaviors, including maternal behavior, aggression, territoriality, social recognition, and social bonding (Freeman and Young, 2013). Elegant rodent studies involving receptor localization, site-specific behavioral pharmacology, viral vector gene manipulations, and transgenic mouse technology have led to the elucidation of the neural mechanisms underlying the effects of these neuropeptides and their receptors on these complex social behaviors (Dölen et al., 2013; Ferguson et al., 2001; Lim et al., 2004b; Owen et al., 2013). Accumulating evidence suggests that OT modulates the neural processing and reinforcing value of social stimuli, which in rodents is primarily olfactory. There is evidence that roles of these peptides are conserved to some degree in humans (Scheele et al., 2013; Skuse et al., 2013), despite differences in the nature of social stimuli between rodent and man.

There has been growing interest in the role of OT in human social cognition (Young and Flanagan-Cato, 2012). Intranasally administered OT (IN-OT) modulates several aspects of social cognition and behavior, including increasing trust, eye-gaze, emotion recognition, empathy and socially reinforced learning (Guastella et al., 2012), and behaviors relevant to pair bonding (Scheele et al., 2013; 2012). Genetic studies also suggest that the OT receptor (OXTR) plays some role in face and emotion recognition and pair bonding behaviors in humans (Skuse et al., 2013; Walum et al., 2012). The OT system is a potential target for enhancing social cognition in psychiatric disorders (Modi and Young, 2012), and several studies have now shown that IN-OT improves some aspects of social functioning in autism spectrum disorder (Andari et al., 2010; Domes et al., 2013; Hollander et al., 2007). Insights into the neural mechanisms of OT action in humans have been gained using brain imaging (Zink and Meyer-Lindenberg, 2012), but inferences on precise mechanisms of action based on these techniques are limited compared to studies using animal models.

Non-human primates (NHP) provide excellent opportunities to explore the neural mechanisms by which OT modulates social cognition and behavior in species that, like humans, rely heavily on visual and auditory cues for social communication. Behavioral studies in NHPs suggest that OT modulates social behaviors related to affiliation, sexual behavior, and pair bonding (A. S. Smith et al., 2010; Snowdon et al., 2010). More recently, IN-OT administration in rhesus macaques has been shown to increase central OT concentrations (Chang et al., 2012) (Modi et al., 2014; Modi, Young, and Parr, *in press*) and to affect a variety of social behaviors including increasing gaze to the eye region of monkey faces (Ebitz et al., 2013), increasing both selfish and altruistic choices to dole out juice rewards (Chang et al., 2012), and changing social visual attentional bias (Ebitz et al., 2013; Parr et al., 2013). As rhesus macaques are amenable to intracranial manipulations (Gothard et al., 2007), including site-specific pharmacology, microdialysis, and electrophysiology,

this species provides an excellent opportunity to explore the precise neural mechanisms by which OT modulates social cognition in primates.

OT and AVP are structurally related peptides that are thought to have arisen early in vertebrate evolution though duplication of an ancestral peptide gene (Acher et al., 1995). The effects of OT and AVP are mediated by four structurally related G-protein coupled receptors, OXTR, AVPR1A, AVPR1B and AVPR2, which themselves are thought to have emerged through gene duplication events. Although the behavioral effects of OT are widely assumed to mediated by central OXTR, OT does cross react with the AVP receptors and *vice versa* (Manning et al., 2012), and some of the behavioral effects of OT are mediated by AVPR1A (Schorscher-Petcu et al., 2010; Song et al., 2013). Only OXTR, AVPR1A, and AVPR1B are expressed in the brain, and most of the social behavioral effects of AVP are mediated by AVPR1A. Homologues of the ancestral OT/AVP peptide are found in invertebrates (Wagenaar et al., 2010), and the *C. elegans* homologue, nemotocin, selectively modulates sensorimotor behaviors associated with mate detection and mating (Garrison et al., 2012). Thus, the role of the OT/AVP system has an evolutionarily conserved role in modulating sociosexual behaviors across behavioral motifs in divergent taxa.

The neuroanatomical localization of OXTR using receptor autoradiography has been useful for identifying neural mechanisms of OT action in rodents (Ferguson et al., 2001; Young and Wang, 2004). Yet, the distribution of OXTR in NHPs has only been described in the common marmoset (Schorscher-Petcu et al., 2009), and more recently in the coppery titi monkey (Freeman et al, *in review*). The pharmacological tools that have been used to map OXTR have failed to yield convincing results in rhesus macaque brain tissue (Toloczko et al., 1997), because the ligands that are highly selective for OXTR in rodents promiscuously bind both OXTR and AVPR1A in primates. In contrast, the neural distribution of AVPR1A in rhesus macaques has previously been described (Young et al., 1999). Therefore, we developed a pharmacologically-informed, competitive-binding protocol for receptor autoradiography that selectively distinguishes OXTR and AVPR1A distributions in primate brain tissue, and we characterized the neuroanatomical distribution of OXTR in rhesus macaque. We also used *in situ* hybridization to localize OXTR mRNA in adjacent sections. Our results provide insights into how OT may modulate the neural processing of and attention to visual and auditory social stimuli and establish a foundation for future mechanistic studies to explore the precise neural mechanisms of OT action in the primate brain.

MATERIALS AND METHODS

Cell culture

To characterize the pharmacological profiles of the ligands to be used in receptor autoradiography, we performed receptor binding assays on membrane preparations from cells expressing either the human OXTR (hOXTR) or the human AVPR1A (hAVPR1A). Two stably transfected Chinese hamster ovary (CHO) cell lines (gifts of Dr. Brian Roth, NIMH Psychoactive Drug Screening Program and UNC-Chapel Hill) were used. These cell lines served as proxies for rhesus receptors binding profiles, as the homology between the rhesus and human OXTR and AVPR1A amino acid sequences are high (>97%) (Salvatore et

al., 1998; Young et al., 1999). Cells were cultured in 75 cm^2 flasks (Corning; Manassas, VA) in an incubator at 37°C, 100% humidity, 5% CO_2, in sterile, filtered Ham's F-12 media (GIBCO; Grand Island, NY) with 10% fetal bovine serum (Hyclone; Waltham, MA), 1% Pen/Strep (GIBCO; Grand Island, NY), 15 mM 1X HEPES buffer solution (GIBCO; Grand Island, NY), and 400 μg/mL of the selection agent G418 sulfate (cellgro; Manassas, VA), which ensures growth of only the cells expressing the gene of interest. Cells were passaged with trypsin when they reached ~80% confluency. A line of untransfected control CHO cells (gift of Dr. Randy Hall, Emory University) were also cultured in the same way, but without the selection agent G418 sulfate.

Membrane Preparation & Protein Quantification

After cells reached confluency in 6-well plates, the media was removed, and 1 mL sterile PBS (pH 7.4) was added to each well. Cells were harvested with a cell scraper and pipetted into centrifuge tubes on ice. Cells were centrifuged for 5 min at 2,000 rpm at 4°C. The next four steps were repeated twice: the supernatent was removed; 500 mL of ice cold Buffer A (50 mM Tris-HCl, 5 mM $MgCl_2$, pH 7.4) was added; cells were homogenized (Cole-Parmer LabGEN 125 homogenizer) on medium speed for approximately 10 sec; finally, cells were ultracentrifuged for 10 min at 44,000 rpm at 4°C. After the second ultracentrifugation, the supernatent was removed, and 355 mL of Buffer A was added. Protein in the membrane samples was quantified using the Pierce BCA Protein Assay Kit according to the kit's instructions (Thermo Scientific). Diluted BSA standards were made using Buffer A as the diluent. The remaining membranes were prepared for freezing so that the final volume was 500 mL and final buffer concentrations were: 1 mg/mL BSA, 5 mM $MgCl_2$, and 1X cOmplete, EDTA-free protease inhibitor (Roche Applied Science, Indianapolis). Aliquoted samples were frozen at -20°C.

Ligand Binding Assays: General Procedure

All reactions took place in 200 mL Buffer B (50 mM Tris-HCl, 5 mM $MgCl_2$, 1 mg/ml BSA, pH 7.4). Reactions were initiated by adding 3 μg of protein (based on an optimization experiment) from the membrane preparations to each reaction tube. Reactions were incubated for 1 hr at RT, rapidly vacuum-filtered using a Brandel Cell Harvester onto Whatman GF/C filter paper that was soaked for 4 hours in 10 mg/ml BSA, and then washed three times with Buffer A (4°C). The radioactivity of the filter paper was quantified using a gamma counter. All reactions in each assay were performed in triplicate, and each set of triplicate values was averaged. Outliers were removed using the Grubbs test (critical Z = 1.15; two-sided alpha set to 0.01). Two independent replications of each assay were performed.

Saturation Binding Assay

Saturation binding assays were performed in order to determine the binding affinity (measured by the dissociation constant, K_d) of the two commercially available radioligands: the OXTR radioligand, ^{125}I-ornithine vasotocin analog (^{125}I-OVTA), and the AVPR1A radioligand, ^{125}I-linear vasopressin-1a antagonist (^{125}I-LVA) (Perkin Elmer; Waltham, MA). Both of these radioligands were tested for their ability to saturate both receptors. Eleven increasing concentrations of each radioligand were tested: 0.008, 0.016, 0.024,

0.031, 0.046, 0.062, 0.093, 0.125, 0.187, 0.250, and 0.500 nM. Average values of non-specific binding determined in the presence of either 1 ! M OT (for hOXTR) or 1 ! M AVP (for hAVPR1A) were subtracted from average total binding to give a measure of specific binding. Nonlinear regression analyses for one-site saturation binding were performed on the resulting specific binding data using GraphPad Prism 5.0 (San Diego, CA) in order to determine K_d.

Competitive Binding Assay

We tested two small molecule, non-peptide ligands that were developed specifically for use in human tissue for their ability to displace radioligand binding to hOXTR and hAVPR1A: a novel OXTR antagonist developed in our lab (ALS-II-69; A. L. Smith et al., 2013a) and an AVPR1A antagonist developed by Sanofi Recherche (SR49059; Gal et al., 1993). SR49059 was purchased from Tocris (Minneapolis, MN). Twelve different increasing concentrations of each competitor were tested: 10^{-13}, 10^{-11}, 10^{-10}, $10^{-9.5}$, 10^{-9}, $10^{-8.5}$, 10^{-8}, $10^{-7.5}$, 10^{-7}, $10^{-6.5}$, 10^{-6}, and 10^{-5} M. AVPR1A compounds were tested for their ability to displace ^{125}I-OVTA from each receptor type. OXTR compounds were tested for their ability to displace ^{125}I-LVA from each receptor type. The concentrations of the radioligands were held constant at the radioligand's K_d for the receptor in use (determined by the saturation experiments above). Nonlinear regression analyses for one-site competition binding were performed using GraphPad Prism 5.0 (San Diego, CA) in order to determine K_i

Tissue preparation and sectioning

Rhesus macaque brains (n=9 males; mean age=1.93 years; age range=1.04–8.77 years) were removed promptly after death, rinsed with PBS, and blocked into three or four coronal blocks, which were then allowed to freeze completely while laying flat on a foil covered slab of dry ice, wrapped tightly in foil, and placed at -80°C until sectioning. Brain blocks were brought up to -20°C then sectioned at 20 μm on a cryostat and mounted on Fisher Frost-plus slides. Slides were stored in a sealed slide box with desiccant and kept at -80°C until use for receptor autoradiography or *in situ* hybridization. Although we had tissue from nine animals, we did not analyze all brain regions from all nine animals. Sections ranged from frontal cortex through the hypothalamus and temporal lobe, and to the cerebellum and brainstem.

Receptor autoradiography

Sections were allowed to thaw in the sealed slide box containing a desiccant packet for 1 hour at 4°C followed by 1 hour at RT in a vacuum desiccator. The slides were processed for OXTR and AVPR1A receptor autoradiography as described previously, with slight modifications (Lim et al., 2004a). Specifically, sections were incubated with either the OXTR radioligand ^{125}I-ornithine vasotocin analog (^{125}I-OVTA) or the AVPR1A radioligand ^{125}I-linear vasopressin antagonist (^{125}I-LVA), at concentrations determined from saturation binding assays to equal the radioligand's K_d for the receptor of interest. Sets of three adjacent sections were incubated in three different conditions: radioligand alone, radioligand plus SR49059 (Tocris, Minneapolis, MN), or radioligand plus ALS-II-69. SR49059 is a small molecule selective antagonist for the human AVPR1A (Gal et al., 1993),

while ALS-II-69 is a small molecule selective antagonist for the human OXTR (A. L. Smith et al., 2013b). These unlabeled competitors were incubated at concentrations that were determined by competitive binding assays to be ideal for selective binding to the receptor of interest. The slides were exposed to BioMax MR film (Kodak, Rochester, NY) for 8 days, then developed. Digital images were obtained from the films using a light box and a SPOT camera (Diagnostic Instruments, Sterling Heights, MI) connected to a computer. Brightness and contrast of the images were equally adjusted for all the sections using Adobe Photoshop (San Jose, CA). Images were compared with a rhesus macaque brain atlas (Paxinos et al., 1999) to identify brain regions.

In situ hybridization

Probes derived from cDNAs encoding the human OXTR and AVPR1A were used for *in situ* hybridization for the rhesus monkey brains. The human OXTR fragment, corresponding to nucleotide 631 to 1751 of human OXTR mRNA (NM_000916.3), and the human AVPR1A fragment, corresponding to nucleotide 2014 to 3198 of human AVPR1A (NM_000706.4), were amplified from human OXTR and AVPR1A plasmids (gifts of Dr. Bice Chini), respectively, using polymerase chain reaction (PCR) and a forward primer (5'-GGAAGATTTAGGCGAGTCCTTCCACA-3') and reverse primer (5'-CCGTACTGTTTGTTGGGCTTCGATTG-3') for AVPR1A and a forward primer (5'-CGCGCTCGCAGCCAACTGGA-3') and reverse primer (5'-TGCGATGGCTCAGGACAAAGGA-3') for OXTR. The hAVPR1A probe was 97% homologous to the rhesus AVPR1A mRNA sequence (XM_001116798.2) and the hOXTR probe was 97% homologous to the rhesus OXTR mRNA sequence (NM_001044732.1). PCR products were inserted to pCRII vector (Invitrogen, Grand Island, NY). ^{35}S-UTP labeled sense and antisense probes were generated from linearized plasmids using T7 or SP6 RNA polymerases.

Sections were allowed to thaw as described above, then hybridized with the probes and washed as described previously with minor modifications (Inoue et al., 2013). Specifically, the length of the proteinase K treatment was increased from 2 min to 6 min, and the parameters for the high stringency wash step were changed as follows: 5% beta-mercaptoethanal was added to the 50% formamide/2x standard sodium citrate solution, and the temperature for this wash step was decreased from 65°C to 62.5°C. The sections were then exposed to BAS-IP TR 2025 E phosphorimaging screens (FujiFilm, Tokyo) for 28 days and then to BioMax MR film (Kodak, Rochester, NY) for 100 days. Phosphorimaging screens were analyzed using a BAS5000 phosphorimager (FujiFilm, Tokyo). After film development, digital images were obtained from the films using a light box and a SPOT camera (Diagnostic Instruments, Sterling Heights, MI) connected to a computer. Brightness and contrast of the images are equally adjusted for all the sections using Adobe Photoshop (San Jose, CA).

RESULTS

Pharmacologically informed design of a competitive binding protocol for OTR autoradiography

Saturation binding assays revealed that both ^{125}I-LVA and ^{125}I-OVTA have subnanomolar affinities for both of the human receptors (Figure 1A-D). ^{125}I-LVA binds to hAVPR1A with a higher affinity (K_d = 30 ± 3.1 pM) than it binds to hOXTR (K_d = 590 ± 450 pM). Similarly, ^{125}I-OVTA binds to hOXTR with a higher affinity (92 ± 18 pM) than it binds to hAVPR1A (360 ± 51 pM). These data suggest that these radioligands exhibit less selectivity for the respective human receptors compared to rodent receptors. Based on these data we used 30 pM for ^{125}I-LVA and 90 pM for ^{125}I-OVTA for receptor autoradiography in rhesus tissue. Using competitive binding assays, we determined the concentrations of unlabeled competitors that would yield maximum selective binding (i.e would compete most of the ^{125}I-OVTA off of AVPR1A without significantly competing the radioligand off of OXTR).

Next we used competitive binding assays to determine the binding affinities (measured by the dissociation constant, K_i) and selectivity profiles of one OXTR ligand and one AVPR1A ligand. The binding curves that result can be compared to determine the ideal concentration at which a majority of binding to one receptor is displaced, but the binding to the other receptor is unaffected. For the AVPR1A competitor SR49059, whose use to selectively occupy AVPR1A in a competitive binding approach has been suggested previously (Ala et al., 1997), we determined that the best concentration for SR49059 to bind to displace ^{125}I-OVTA from hAVPR1A without affecting binding to hOXTR is 10 nM (Figure 1E). The OXTR antagonist ALS-II-69 is extremely selective for the human OXTR, and it only barely begins to displace ^{125}I-LVA from the hAVPR1A at concentrations higher than 1 μM (Figure 1F). Therefore, concentrations of ALS-II-69 up to 1 μM could be used to displace binding to OXTR without affecting the binding to AVPR1A. In order to keep the concentrations of these two competitors relatively consistent, we set both in the same order of magnitude: 10 nM SR49059 and 20 nM ALS-II-69.

Based on these *in vitro* results, our pharmacologically informed, competitive binding receptor autoradiography protocol is: a) radioligand alone (30 pM ^{125}I-LVA or 90 pm ^{125}IOVTA), b) radioligand plus 10 nM SR49059 to selectively block AVPR1A, and c) radioligand plus 20 nM ALS-II-69 to selectively block OXTR.

Competitive Binding Receptor Autoradiography

In the absence of unlabeled competitors, ^{125}I-OVTA and ^{125}I-LVA produced similar binding patterns in rhesus macaque brain tissue (Figure 2), which is consistent with what was previously reported for these radioligands in this species (Toloczko et al., 1997; Young et al., 1999). Dense binding was detected in the anterior cingulate cortex (ACC), bed nucleus of stria terminalis (BNST), central amygdala (CeA), claustrum (Cl), entorhinal cortex (Ent), infundibulum (Inf), insular cortex (Ins), median eminence (ME), parasubiculum (PASB), and subiculum (SB) (Figure 1, black arrows). Our results with ^{125}I-LVA fully match the previously reported distribution of AVPR1A binding in the rhesus

macaque (Young et al, 1999). There are some areas with very low levels of ^{125}I-OVTA binding that do not seem to overlap with ^{125}I-LVA binding, for example in the nucleus basalis of Meynert (NBM) and ventromedial hypothalamus (VMH) (Figure 3, white arrows), but it is difficult to assess with certainty if this signal is specific OXTR binding.

When the selective OXTR competitor ALS-II-69 was co-incubated on the tissue at a concentration determined from pharmacological assessments to selectively occupy OXTR without binding to AVPR1A, it did not reduce the overall levels of binding in the most intensely labeled areas for either radioligand (Figure 3E,F) compared to the radioligand alone condition (Figure 3A,B). Therefore, the majority of binding from ^{125}I-OVTA is not due to OXTR binding. In contrast, the selective AVPR1A competitor SR49059, when used at a concentration that binds to AVPR1A without significantly binding to OXTR, drastically reduced binding of both ^{125}I-LVA and ^{125}I-OVTA in most brain regions (Figure 3C,D). Co-incubation with both OXTR and AVPR1A competitors resulted in binding patterns indistinguishable from that of the AVPR1A competitor alone for the areas of densest binding (not shown), making colocalization of AVPR1A and OXTR unlikely.

It should be noted that the small molecule competitors did not eliminate the areas of high density specific binding at the concentrations used, which is likely due to the fact that the small, nonpeptide competitors can act as allosteric modulators to affect the affinity of the orthosteric ligand (in our case, the peptide radioligand) without directly competing it off of the putative ligand-binding pocket (Gruber et al., 2010). Alternatively, the areas of residual binding in the presence of a competitor(s) may also reflect the differences in binding kinetics between the radioligands (with pM affinities) and the competitors (with nM affinities). Thus, the residual binding likely represents *bona fide* AVPR1A binding rather than non-specific binding, and the overall binding pattern from both radioligands in the alone condition is likely due to AVPR1A binding. Furthermore, this competitive approach revealed a few brain regions with modest levels of ^{125}I-OVTA binding and no binding from ^{125}I-LVA, including NBM (Figure 3B,D, white circles). However, the overall signal that remains for OXTR in the presence of SR49059 (Figure 3D) is very light and difficult to interpret with confidence.

In situ hybridization confirms OXTR expression

We used adjacent sections from the same individual for *in situ* hybridization for OXTR and AVPR1A mRNA and compared the resulting signals for AVPR1A mRNA and OXTR mRNA to the pattern of binding produced by ^{125}I-OVTA alone (Figure 4). In contrast to radioligand binding patterns, the distribution of AVPR1A and OXTR mRNAs were non-overlapping (Figure 4B,C). Furthermore, the binding pattern produced by the AVPR1A antisense probe matched the binding of ^{125}I-OVTA in the BNST, CeA, Ent, Inf, PASB, and presubiculum (PSB) (Figure 4A,B, black arrows). In contrast, the binding pattern produced by the OXTR mRNA antisense probe resulted in a signal in the NBM and VMH, which matched areas of modest binding from ^{125}I-OVTA alone (Figure 4A,C, white arrows). OXTR sense strand probes were used to distinguish the mRNA signal from nonspecific binding of the probes, which was apparent in the hippocampus (Hipp) (Figure 4C,D, gray arrows).

By comparing the binding signals from OXTR protein and OXTR mRNA to acetycholinesterase (AChE) counterstained sections and a published rhesus macaque brain atlas (Paxinos et al., 1999), we were able to confidently identify areas of OXTR expression in the rhesus macaque brain. The overall expression of OXTR in the rhesus brain (Figure 5) is significantly more restricted than AVPR1A, with a clear, consistent signal detected in five areas of the brain—NBM, the peduncopontine tegmental nucleus (PPT), the superficial gray layer of the superior colliculus (SuG), the trapezoid body (TB) and the VMH. Comparison of OXTR mRNA with AChE staining in sections containing the NBM and PPT clearly demonstrates that the OXTR mRNA producing cells are confined predominately to the cholinergic regions that anatomically distinguish NBM and PPT from their respective surrounding areas (Figure 6). While it is not likely that these five areas are the only regions that express OXTR, these are the areas with densities of mRNA high enough to be detectable by the current methods.

DISCUSSION

Here we provide the first demonstration of the distribution of OXTR binding and mRNA in the rhesus macaque brain. These results provide important insights into the neural mechanisms of OT action in the rhesus macaque. Our results suggest that the highest areas of expression are the NBM, PPT, SuG, TB, and VMH. In contrast to in the rodent, where OXTR expression is abundant in regions processing olfactory information, OXTR in the macaque is present in regions processing visual and auditory information. Here we will discuss the functional significance of each region separately.

Nucleus basalis of Meynert and pedunculopontine tegmental nucleus: visual attention and cholinergic innervation of the brain

The NBM is a highly interconnected area of the basal forebrain that provides cholinergic innervation into the entire neocortex and basolateral amygdala. This cholinergic input from NBM plays a critical role in selective attention, attentional effort, and motivation, specifically with respect to visual attention (Muir et al., 1993). Thus, OXTR activation in this region of the rhesus macaque brain likely influences visual attention to social cues. A recent study reported that IN-OT in rhesus macaques changes the visual social attentional bias toward emotional faces, and the authors suggest a role for OT in “the earliest stages of social information processing” (Ebitz et al., 2013). Furthermore, Chang and colleagues also support the hypothesis that OT modulates selective attention and have said that their findings “invite the possibility that OT gates the activity of attention circuits in the brain specifically during active interaction with others”, perhaps via action at OXTR in the NBM (Chang et al., 2012).

We also detected modest OXTR mRNA in the PPT, which is another highly interconnected region of the brain that has been implicated in a variety of functions, including sleep, locomotion, reaction time, reinforcement learning, sensation, attention, and consciousness (Winn, 2006). This nucleus is made up of a cholinergic and a non-cholinergic subdivision. The cholinergic subdivision, where we see OXTR expression, is the major source of cholinergic input to the midbrain and one of the major ascending arousal pathways in the

brainstem (Kobayashi et al., 2002). The localization of OXTR in the cholinergic subdivision of the PPT is reminiscent of OXTR expression in the NBM (Figure 6), and cholinergic input from the PPT strongly innervates the macaque superior colliculus (SC)(Ma et al., 1991). Neurons in the PPT have also been shown to be active in monkeys during saccade tasks (Okada and Kobayashi, 2009) and to directly stimulate SC neurons and facilitate the initiation of saccadic eye movements (Kobayashi et al., 2001). Thus, it is possible that these OT-sensitive cholinergic areas could be mediating some aspects of the changes in eye movements and shifts in visual attention in response to changing social cues in the environment.

Superior colliculus: visual and multimodal processing and gaze control

The SC in rhesus macaques is involved in the control of eye movements and visual attention (Wurtz and Goldberg, 1972). OXTR mRNA and binding were most dense in the superficial gray layer of the SC (SuG). The SuG receives input from the retina, is organized to contain a map of visual space (Goldberg and Wurtz, 1972), and is thought to provide synaptic input to the deeper layers of the SC in order to mediate orienting movements in response to specific visual cues (Ma et al., 1991). Thus it is plausible to hypothesize that OXTR in SuG could modulate visually guided orienting responses to socially relevant stimuli detected in visual space. In a recent study that examined the effects of IN-OT on altruistic reward allocation in macaques, treatment with OT selectively increased the donor monkey's attention toward the passive recipient monkey only after the altruistic reward delivery; the authors suggest that perhaps this effect is due to OT's influence on “neural circuits mediating orienting behavior, including... [the] superior colliculus” (Chang et al., 2012). Indirect support for this idea comes from an IN-OT study in humans that reported increased functional coupling between the SC and the amygdala during a face viewing task (Gamer et al., 2010).

Trapezoid body: auditory input from the cochlea

OXTR was detected in the TB of the brainstem, which receives synaptic input from the cochlear nucleus (Borst and Soria van Hoeve, 2012). The characteristics of the connectivity between the TB and other regions in the auditory pathway are considered to underlie the ability to localize sound sources in space (Schneggenburger and Forsythe, 2006). It is speculative at best to suggest a function of OXTR in this fast-acting auditory relay nucleus, but given the macaque's use of vocal communication by both infants and adults in a variety of social settings, it is plausible that OT may have a neuromodulatory effect on brain regions involved in the earliest stages of auditory processing, which may influence the processing of vocal communication. In humans, IN-OT affects the reaction to infant cries (Bakermans-Kranenburg et al., 2012) and infant laughter (Riem et al., 2012) and may even play a role in navigating the “cocktail party effect” (Tops et al., 2011), which is the phenomenon whereby an individual can focus one's auditory attention on one particular stimulus and “tune out” other competing stimuli, such as being able to follow a single conversation in a crowded, noisy room. In fact, it has been suggested that the cocktail party effect requires binaural processing of sound (Hawley et al., 2004) and is related to the ability to localize sound in space (Fritz et al., 2007), which further supports the importance of the TB in this purportedly OT-sensitive ability.

Ventromedial hypothalamus: sexual behavior and feeding

OXTR binding has been found in VMH in mice, rats, guinea pigs, prairie and montane voles, two species of Central America singing mice, and two species of the South American rodent the tuco-tuco (Beery et al., 2008). Thus, the VMH may represent one of the most evolutionarily conserved regions of OXTR expression across mammals. In rats, OXTR in the VMH regulate female sexual receptivity in an estrogen (E2) dependent manner (Bale et al., 2001; McCarthy et al., 1994). In primates, female rhesus macaque sexual behavior is highest during the peak in E2 during estrous and increases after estrogen treatment in ovariectomized rhesus macaques (Zehr et al., 1998). Thus, it is possible that OXTR in the VMH plays a conserved role in regulating sexual behavior in rodents and primates. There is also evidence that OXTR in the VMH also play a role in the motivational switching between sexual behavior and feeding in rodents (Leng et al., 2008) and thus may have a role in regulating food intake and appetite in primates as well.

Comparison to OXTR expression in other primate species

To our knowledge, central OXTR distribution has only been mapped in three other primate species: the common marmoset (*Callithrix jacchus*)(Schorscher-Petcu et al., 2009), the coppery titi monkey (*Callicebus cupreus*)(Freeman et al, *in review*) and the human (*Homo sapiens*)(Loup et al., 1991). However, none of these studies, except the titi monkey study from our group, used *in situ* hybridization; both of the others relied only on receptor autoradiography. While the human and marmoset studies used at least three different concentrations of various unlabeled competitors to establish specificity of ^{125}I-OVTA binding, these concentrations were arbitrary and, in the case of the human brain, extremely high. Thus, while the results of these two studies are slightly tenuous due to the aforementioned issues of radioligand specificity and displacer selectivity, the results are still worth evaluating in light of the current study.

There were only two areas of consistent OXTR binding across all four primate species: NBM and SC (Loup et al., 1991; Schorscher-Petcu et al., 2009; Freeman et al, *in review*). Clear OXTR binding in the NBM has been reported for human brain and, in the current study, for rhesus macaque brain. In marmosets, the authors labeled an area of OXTR expression in the basal forebrain as the diagonal band of Broca (DB), but in marmoset brain tissue, the DB is very near to the NBM, and based on a replication experiment performed in our lab, we feel that this region is in fact the NBM and not the DB (Freeman, unpublished data). OXTR binding was also clearly evident in the NBM of the coppery titi monkey (Freeman et al, *in review*). The rhesus macaque and the marmoset both express dense OXTR in the SuG, and in the human and titi monkey, OXTR binding was detected in the SC without distinguishing layers. Thus, the NBM and SC represent conserved regions of OXTR expression across primate species and may play similar roles mediating social attention and gaze direction.

As described above, rhesus macaques and most other species that have been investigated for OXTR binding have OXTR expression in the VMH. Quite unexpectedly, marmosets do not express OXTR in the VMH, but they do have AVPR1A binding in this region, which suggests that OT could be acting there via AVPR1A in this species (Schorscher-Petcu et al.,

2009). In the human and titi monkey brain, no OXTR or AVPR1A binding was reported for VMH (Loup et al., 1991; Freeman et al., *in review*). Thus, while OXTR in VMH in rhesus macaques resembles the majority of mammalian species, there are some differences across primates.

Two publications have used immunohistochemistry (IHC) with an OXTR antibody to identify areas of OXTR expression in the macaque brain (Boccia et al., 2001) and in human brain tissue (Boccia et al., 2013). However using IHC to stain for OXTR has been notoriously problematic; a study that tested six different OXTR antibodies found that all of them produced identical patterns of staining in brain tissue from wildtype and OXTR knockout mice, indicating their unreliability in detecting OXTR in rodent brain (Yoshida et al., 2009). While the antibody used in the Boccia et al. publications was not included in the six that were tested by Yoshida et al, neither the human or the macaque IHC paper confirmed specificity of the antibody in brain tissue (uterus tissue was used in the human IHC paper) or with *in situ* hybridization or with mouse brain tissue from OXTR knock out and wildtype strains.

While the expression of OXTR among the four primates examined thus far is conserved in the NBM and SC, the species differences in OXTR are perhaps more striking. For example, the monogamous marmoset has dense OXTR binding in the nucleus accumbens not found in the other primates. Likewise, the monogamous titi monkey has the densest OXTR binding in the hippocampus and presubiculum, in contrast to the other primates. Thus, while there is an evolutionarily conserved core element of OXTR binding in regions involved in social visual attention and gaze, there is a remarkable richness in diversity in expression that could be related to behavioral specialization in each species. A similar diversity in OXTR expression in found in rodents, as voles, mice, and rats each have unique distributions of OXTR binding (Burbach et al., 2006; Olazábal and Young, 2006). Thus the element of phylogenetic diversity that is a hallmark of OXTR expression in rodents is conserved in primates.

It is noteworthy that in rodents, OXTR is concentrated in brain regions directly processing olfactory information, including the olfactory bulb, piriform cortex, and medial amygdala (Ferguson 2001). In contrast, in the rhesus macaque, OXTR is most robustly expressed in cholinergic regions that modulate other brain regions, such as the cerebral cortex and basolateral amygdala, which may influence social behavioral processes. Thus, while OT may directly affect the perception and processing of olfactory social cues in rodents, in the primate OT may modulate social behavior by modulating cholinergic input to brain regions involved in higher order neural processing.

Perspectives on oxytocin function and considerations for future research

It should be noted that we describe here with confidence the brain regions with the highest levels of OXTR expression and binding. However, we acknowledge that OT may modulate OXTR fields not detectable using the techniques used here. For example, OXTR on serotonergic terminals in the nucleus accumbens from projections arising in the dorsal raphe have recently been shown to modulate social reward in mice (Dölen et al., 2013), even though receptor autoradiography suggests that the mouse nucleus accumbens is devoid of OXTR. Thus, it is likely that OT may be acting on terminals of projections of the regions in

which OXTR mRNA was detected. For example, the NBM projects heavily to the basolateral amygdala and cerebral cortex, though OXTR binding was not evident in these areas in the present study. Electrophysiological studies are needed to reveal whether OT significantly modulates activity in these regions by modulating presynaptic inputs from the NBM.

It is notable that while limbic brain region in rodents richly express OXTR, binding and mRNA for OXTR binding is largely absent in the limbic system in rhesus macaques. However, we do not conclude that the limbic system in the macaque is unresponsive to OT, as OXTR may be expressed at levels below detection or may be primarily on synaptic terminals as described above and thus avoid detection by autoradiography and *in situ* hybridization. Furthermore, previous studies have reported that the density of OXTR expression does not correlate with electrophysiological responses to OT, as brain regions with low OXTR binding often display greater responses to OT than those with dense binding (Terenzi and Ingram, 2005; Wilson et al., 2005).

A final consideration is that the broader and greater intensity of AVPR1A binding relative to OXTR, along with the cross-reactivity of OT with AVPR1A raises the possibility that OT regulates social cognition and behavior through complex interactions with both receptors. This would provide a mechanism by which OT could have one set of actions under conditions of low OT concentrations through actions on OXTR, and a different set of actions at higher concentrations through activation of AVPR1A. Thus, it may be more appropriate to consider OXTR and AVPR1A as two subtypes of neurohypophyseal peptide receptors, and some of the effects of IN-OT may be attributable to AVPR1A activation (Young and Flanagan-Cato, 2012). Future behavioral pharmacology studies in nonhuman primates should incorporate selective OXTR and AVPR1A antagonists, such as those used as selective competitors in the present study, to determine the contribution of each receptor to OT-mediated changes in behavior and physiology.

Conclusion

By using a combination of *in situ* hybridization and competitive binding autoradiography with selective ligands, it is possible to establish the distribution of OXTR expression in primate brain tissue, a task that has remained a lingering challenge due to the previously described issues in ligand selectivity. While the distribution of OXTR in the rhesus macaque likely contributes to a variety of functions, such as auditory processing, sexual behavior, and feeding, it is noteworthy that OXTR expression in this species is abundant in areas of the brain that modulate visual attention and orienting responses to visual and auditory stimuli—functions that are critical in a species that uses visual and auditory cues as the primary modalities for social communication, in order to appropriately interpret and subsequent respond to species-typical social behavior.

Research examining the impact of OT on the behavior of humans and NHP will undoubtedly continue to progress, and the results of this study should be useful for informing the experimental design and interpretation of future studies and ultimately contribute to a more complete understanding of the neurophysiology of the OT system in primates.

Acknowledgments

We would like to thank Dr. Randy Hall for advise on the pharmacology experiments and Dr. Todd Preuss for his advice on primate neuroanatomy. We would also like to thank Dr. Brian Roth of NIMH Psychoactive Drug Screening Program and UNC Chapel Hill for generously providing the stably infected human OXTR and AVPR1a CHO cell lines and Dr. Bice Chini from CNR Institute of Neuroscience, Milan, Italy for providing the human OXTR and AVPR1a plasmids. Our gratitude also goes to the veterinary, pathology, and animal care staff members at Yerkes National Primate Research Center, especially to Carmen Nash for her assistance with this project.

FUNDING

This work was supported by NIH grants MH090776 and 1P50MH100023 to L.J.Y. Training support for S.M.F was provided by T32MH073525-06. Additional support was provided by Office of Research Infrastructure Programs/OD P51OD011132 (formerly NCRR P51RR000165) to YNPRC.

REFERENCES

Acher R, Chauvet J, Chauvet MT. Man and the chimaera. Selective versus neutral oxytocin evolution. Adv. Exp. Med. Biol. 1995; 395:615–627. [PubMed: 8714026]

Ala Y, Morin D, Mahé E, Cotte N, Mouillac B, Jard S, Barberis C, Tribollet E, Dreifuss JJ, Sawyer WH, Wo NC, Chan WY, Kolodziejczyk AS, Cheng LL, Manning M. Properties of a new radioiodinated antagonist for human vasopressin V2 and V1a receptors. Eur. J. Pharmacol. 1997; 331:285–293. [PubMed: 9274991]

Andari E, Duhamel J-R, Zalla T, Herbrecht E, Leboyer M, Sirigu A. Promoting social behavior with oxytocin in high-functioning autism spectrum disorders. Proceedings of the National Academy of Sciences. 2010; 107:4389–4394.

Bakermans-Kranenburg MJ, van IJzendoorn MH, Riem MME, Tops M, Alink LRA. Oxytocin decreases handgrip force in reaction to infant crying in females without harsh parenting experiences. Soc Cogn Affect Neurosci. 2012; 7:951–957. [PubMed: 22037689]

Bale TL, Davis AM, Auger AP, Dorsa DM, McCarthy MM. CNS region-specific oxytocin receptor expression: importance in regulation of anxiety and sex behavior. J. Neurosci. 2001; 21:2546–2552. [PubMed: 11264328]

Beery AK, Lacey EA, Francis DD. Oxytocin and vasopressin receptor distributions in a solitary and a social species of tuco-tuco (Ctenomys haigi and Ctenomys sociabilis). J. Comp. Neurol. 2008; 507:1847–1859. [PubMed: 18271022]

Boccia ML, Panicker AK, Pedersen C, Petrusz P. Oxytocin receptors in non-human primate brain visualized with monoclonal antibody. Neuroreport. 2001; 12:1723–1726. [PubMed: 11409747]

Boccia ML, Petrusz P, Suzuki K, Marson L, Pedersen CA. Immunohistochemical localization of oxytocin receptors in human brain. Neuroscience. 2013; 253:155–164.. [PubMed: 24012742]

Borst JGG, Soria van Hoeve J. The calyx of held synapse: from model synapse to auditory relay. Annu. Rev. Physiol. 2012; 74:199–224. [PubMed: 22035348]

Burbach JP, Young LJ, Russell JA. Oxytocin: Synthesis, Secretion, and Reproductive Function. Knobil and Neill's physiology of reproduction. 2006:3055–3126.

Chang SWC, Barter JW, Ebitz RB, Watson KK, Platt ML. Inhaled oxytocin amplifies both vicarious reinforcement and self reinforcement in rhesus macaques (Macaca mulatta). Proceedings of the National Academy of Sciences. 2012; 109:959–964.

Domes G, Heinrichs M, Kumbier E, Grossmann A, Hauenstein K, Herpertz SC. Effects of intranasal oxytocin on the neural basis of face processing in autism spectrum disorder. Biological Psychiatry. 2013; 74:164–171. [PubMed: 23510581]

Dölen G, Darvishzadeh A, Huang KW, Malenka RC. Social reward requires coordinated activity of nucleus accumbens oxytocin and serotonin. Nature. 2013; 501:179–184. [PubMed: 24025838]

Ebitz RB, Watson KK, Platt ML. Oxytocin blunts social vigilance in the rhesus macaque. Proceedings of the National Academy of Sciences. 2013; 110:11630–11635.

Ferguson JN, Aldag JM, Insel TR, Young LJ. Oxytocin in the medial amygdala is essential for social recognition in the mouse. J. Neurosci. 2001; 21:8278–8285. [PubMed: 11588199]

Freeman, SM.; Young, LJ. Oxytocin, vasopressin, and the evolution of mating systems in mammals. In: Choleris, E.; Pfaff, DW.; Kavaliers, M., editors. Oxytocin, Vasopressin and Related Peptides in the Regulation of Behavior. Cambridge. Cambridge University Press; 2013. p. 128-147.

Freeman SM, Walum H, Inoue K, Smith AS, Goodman MM, Bales KL, Young LJ. Neuroanatomical distribution of oxytocin and vasopressin 1a receptors in the socially monogamous coppery titi monkey (Callicebus cupreus). Neuroscience. in review.

Fritz JB, Elhilali M, David SV, Shamma SA. Auditory attention--focusing the searchlight on sound. Curr. Opin. Neurobiol. 2007; 17:437–455. [PubMed: 17714933]

Gal CS-L, Wagnon J, Garcia C. Biochemical and pharmacological properties of SR 49059, a new, potent, nonpeptide antagonist of rat and human vasopressin V1a receptors. Journal of Clinical Investigation. 1993

Gamer M, Zurowski B, Büchel C. Different amygdala subregions mediate valence-related and attentional effects of oxytocin in humans. Proceedings of the National Academy of Sciences. 2010; 107:9400–9405.

Garrison JL, Macosko EZ, Bernstein S, Pokala N, Albrecht DR, Bargmann CI. Oxytocin/vasopressin-related peptides have an ancient role in reproductive behavior. Science. 2012; 338:540–543. [PubMed: 23112335]

Goldberg ME, Wurtz RH. Activity of superior colliculus in behaving monkey. I. Visual receptive fields of single neurons. J. Neurophysiol. 1972; 35:542–559.

Gothard KM, Battaglia FP, Erickson CA, Spitler KM, Amaral DG. Neural responses to facial expression and face identity in the monkey amygdala. J. Neurophysiol. 2007; 97:1671–1683. [PubMed: 17093126]

Gruber CW, Muttenthaler M, Freissmuth M. Ligand-based peptide design and combinatorial peptide libraries to target G protein-coupled receptors. Curr. Pharm. Des. 2010; 16:3071–3088. [PubMed: 20687879]

Guastella AJ, Graustella AJ, MacLeod C. A critical review of the influence of oxytocin nasal spray on social cognition in humans: evidence and future directions. Hormones and Behavior. 2012; 61:410–418. [PubMed: 22265852]

Hawley ML, Litovsky RY, Culling JF. The benefit of binaural hearing in a cocktail party: effect of location and type of interferer. J. Acoust. Soc. Am. 2004; 115:833–843. [PubMed: 15000195]

Hollander E, Bartz J, Chaplin W, Phillips A, Sumner J, Soorya L, Anagnostou E, Wasserman S. Oxytocin increases retention of social cognition in autism. Biological Psychiatry. 2007; 61:498–503. [PubMed: 16904652]

Inoue K, Burkett JP, Young LJ. Neuroanatomical distribution of μ-opioid receptor mRNA and binding in monogamous prairie voles (Microtus ochrogaster) and non-monogamous meadow voles (Microtus pennsylvanicus). Neuroscience. 2013; 244:122–133. [PubMed: 23537838]

Kobayashi Y, Inoue Y, Yamamoto M, Isa T, Aizawa H. Contribution of pedunculopontine tegmental nucleus neurons to performance of visually guided saccade tasks in monkeys. J. Neurophysiol. 2002; 88:715–731. [PubMed: 12163524]

Kobayashi Y, Saito Y, Isa T. Facilitation of saccade initiation by brainstem cholinergic system. Brain Dev. 23 Suppl. 2001; 1:S24–7.

Leng G, Onaka T, Caquineau C, Sabatier N, Tobin VA, Takayanagi Y. Oxytocin and appetite. Prog. Brain Res. 2008; 170:137–151. [PubMed: 18655879]

Lim MM, Murphy AZ, Young LJ. Ventral striatopallidal oxytocin and vasopressin V1a receptors in the monogamous prairie vole (Microtus ochrogaster). J. Comp. Neurol. 2004a; 468:555–570. [PubMed: 14689486]

Lim MM, Wang Z, Olazábal DE, Ren X, Terwilliger EF, Young LJ. Enhanced partner preference in a promiscuous species by manipulating the expression of a single gene. Nature. 2004b; 429:754–757. [PubMed: 15201909]

Loup F, Tribollet E, Dubois-Dauphin M, Dreifuss JJ. Localization of high-affinity binding sites for oxytocin and vasopressin in the human brain. An autoradiographic study. Brain Res. 1991; 555:220–232. [PubMed: 1657300]

Ma TP, Graybiel AM, Wurtz RH. Location of saccade-related neurons in the macaque superior colliculus. Exp Brain Res. 1991; 85:21–35. [PubMed: 1715825]

Manning M, Misicka A, Olma A, Bankowski K, Stoev S, Chini B, Durroux T, Mouillac B, Corbani M, Guillon G. Oxytocin and vasopressin agonists and antagonists as research tools and potential therapeutics. Journal of Neuroendocrinology. 2012; 24:609–628. [PubMed: 22375852]

McCarthy MM, Kleopoulos SP, Mobbs CV, Pfaff DW. Infusion of antisense oligodeoxynucleotides to the oxytocin receptor in the ventromedial hypothalamus reduces estrogen-induced sexual receptivity and oxytocin receptor binding in the female rat. Neuroendocrinology. 1994; 59:432–440. [PubMed: 8022519]

Modi ME, Connor-Stroud F, Landgraf R, Young LJ, Parr LA. Aerosolized oxytocin increases cerebrospinal fluid oxytocin in rhesus macaques. Psychoneuroendocrinology. 2014

Modi ME, Young LJ. The oxytocin system in drug discovery for autism: animal models and novel therapeutic strategies. Hormones and Behavior. 2012; 61:340–350. [PubMed: 22206823]

Muir JL, Page KJ, Sirinathsinghji DJ, Robbins TW, Everitt BJ. Excitotoxic lesions of basal forebrain cholinergic neurons: effects on learning, memory and attention. Behavioural Brain Research. 1993; 57:123–131. [PubMed: 7509608]

Okada K-I, Kobayashi Y. Characterization of oculomotor and visual activities in the primate pedunculopontine tegmental nucleus during visually guided saccade tasks. Eur J Neurosci. 2009; 30:2211–2223. [PubMed: 20128856]

Olazábal DE, Young LJ. Species and individual differences in juvenile female alloparental care are associated with oxytocin receptor density in the striatum and the lateral septum. Hormones and Behavior. 2006; 49:681–687. [PubMed: 16442534]

Owen SF, Tuncdemir SN, Bader PL, Tirko NN, Fishell G, Tsien RW. Oxytocin enhances hippocampal spike transmission by modulating fast-spiking interneurons. Nature. 2013; 500:458–462. [PubMed: 23913275]

Parr LA, Modi M, Siebert E, Young LJ. Intranasal oxytocin selectively attenuates rhesus monkeys' attention to negative facial expressions. Psychoneuroendocrinology. 2013

Paxinos, G.; Huang, X-F.; Toga, AW. The Rhesus Monkey Brain in Stereotaxic Coordinates. Academic Press; San Diego: 1999.

Riem MME, van IJzendoorn MH, Tops M, Boksem MAS, Rombouts SARB, Bakermans-Kranenburg MJ. No laughing matter: intranasal oxytocin administration changes functional brain connectivity during exposure to infant laughter. Neuropsychopharmacology. 2012; 37:1257–1266. [PubMed: 22189289]

Salvatore CA, Woyden CJ, Guidotti MT, Pettibone DJ, Jacobson MA. Cloning and expression of the rhesus monkey oxytocin receptor. J. Recept. Signal Transduct. Res. 1998; 18:15–24. [PubMed: 9493565]

Scheele D, Striepens N, Güntürkün O, Deutschländer S, Maier W, Kendrick KM, Hurlemann R. Oxytocin modulates social distance between males and females. J. Neurosci. 2012; 32:16074–16079. [PubMed: 23152592]

Scheele D, Wille A, Kendrick KM, Stoffel-Wagner B, Becker B, Güntürkün O, Maier W, Hurlemann R. Oxytocin enhances brain reward system responses in men viewing the face of their female partner. Proceedings of the National Academy of Sciences. 2013; 110:20308–20313.

Schneggenburger R, Forsythe ID. The calyx of Held. Cell Tissue Res. 2006; 326:311–337. [PubMed: 16896951]

Schorscher-Petcu A, Dupré A, Tribollet E. Distribution of vasopressin and oxytocin binding sites in the brain and upper spinal cord of the common marmoset. Neuroscience Letters. 2009; 461:217–222. [PubMed: 19539696]

Schorscher-Petcu A, Sotocinal S, Ciura S, Dupré A, Ritchie J, Sorge RE, Crawley JN, Hu S-B, Nishimori K, Young LJ, Tribollet E, Quirion R, Mogil JS. Oxytocin-induced analgesia and scratching are mediated by the vasopressin-1A receptor in the mouse. J. Neurosci. 2010; 30:8274–8284. [PubMed: 20554879]

Skuse DH, Lori A, Cubells JF, Lee I, Conneely KN, Puura K, Lehtimäki T, Binder EB, Young LJ. Common polymorphism in the oxytocin receptor gene (OXTR) is associated with human social recognition skills. Proceedings of the National Academy of Sciences. 2013

Smith AL, Freeman SM, Voll RJ, Young LJ, Goodman MM. Investigation of an F-18 Oxytocin Receptor Selective Ligand via PET Imaging. Bioorg. Med. Chem. Lett. 2013a

Smith AL, Freeman SM, Voll RJ, Young LJ, Goodman MM. Investigation of an F-18 oxytocin receptor selective ligand via PET imaging. Bioorg. Med. Chem. Lett. 2013b; 23:5415–5420. [PubMed: 23978650]

Smith AS, Ågmo A, Birnie AK, French JA. Manipulation of the oxytocin system alters social behavior and attraction in pair-bonding primates, Callithrix penicillata. Hormones and Behavior. 2010; 57:255–262. [PubMed: 20025881]

Snowdon CT, Pieper BA, Boe CY, Cronin KA, Kurian AV, Ziegler TE. Variation in oxytocin is related to variation in affiliative behavior in monogamous, pairbonded tamarins. Hormones and Behavior. 2010; 58:614–618. [PubMed: 20600045]

Song, EZ.; McCann, KE.; McNeill, JK., IV; Huhman, KL.; Albers, HE. Oxytocin Induces Social Communication in Male Syrian Hamsters by Activating V1a and not OT Receptors.. Presented at the Society for Neuroscience Annual Meeting; San Diego. 2013.

Terenzi MG, Ingram CD. Oxytocin-induced excitation of neurones in the rat central and medial amygdaloid nuclei. NSC. 2005; 134:345–354.

Toloczko DM, Young LJ, Insel TR. Are there oxytocin receptors in the primate brain? Annals of the New York Academy of Sciences. 1997; 807:506–509. [PubMed: 9071384]

Tops M, van IJzendoorn MH, Riem MME, Boksem MAS, Bakermans-Kranenburg MJ. Oxytocin receptor gene associated with the efficiency of social auditory processing. Front Psychiatry. 2011; 2:60. [PubMed: 22069391]

Wagenaar DA, Hamilton MS, Huang T, Kristan WB, French KA. A hormone-activated central pattern generator for courtship. Curr. Biol. 2010; 20:487–495. [PubMed: 20226670]

Walum H, Lichtenstein P, Neiderhiser JM, Reiss D, Ganiban JM, Spotts EL, Pedersen NL, Anckarsäter H, Larsson H, Westberg L. Variation in the oxytocin receptor gene is associated with pair-bonding and social behavior. Biological Psychiatry. 2012; 71:419–426. [PubMed: 22015110]

Wilson BC, Terenzi MG, Ingram CD. Differential excitatory responses to oxytocin in sub-divisions of the bed nuclei of the stria terminalis. Neuropeptides. 2005; 39:403–407. [PubMed: 15975651]

Winn P. How best to consider the structure and function of the pedunculopontine tegmental nucleus: evidence from animal studies. J. Neurol. Sci. 2006; 248:234–250. [PubMed: 16765383]

Wurtz RH, Goldberg ME. The primate superior colliculus and the shift of visual attention. Invest Ophthalmol. 1972; 11:441–450. [PubMed: 4624290]

Yoshida M, Takayanagi Y, Inoue K, Kimura T, Young LJ, Onaka T, Nishimori K. Evidence that oxytocin exerts anxiolytic effects via oxytocin receptor expressed in serotonergic neurons in mice. J. Neurosci. 2009; 29:2259–2271. [PubMed: 19228979]

Young LJ, Flanagan-Cato LM. Editorial comment: oxytocin, vasopressin and social behavior. Hormones and Behavior. 2012; 61:227–229. [PubMed: 22443808]

Young LJ, Toloczko D, Insel TR. Localization of vasopressin (V1a) receptor binding and mRNA in the rhesus monkey brain. Journal of Neuroendocrinology. 1999; 11:291–297. [PubMed: 10223283]

Young LJ, Wang Z. The neurobiology of pair bonding. Nat. Neurosci. 2004; 7:1048–1054. [PubMed: 15452576]

Zehr JL, Maestripieri D, Wallen K. Estradiol increases female sexual initiation independent of male responsiveness in rhesus monkeys. Hormones and Behavior. 1998; 33:95–103. [PubMed: 9647935]

Zink CF, Meyer-Lindenberg A. Human neuroimaging of oxytocin and vasopressin in social cognition. Hormones and Behavior. 2012; 61:400–409. [PubMed: 22326707]

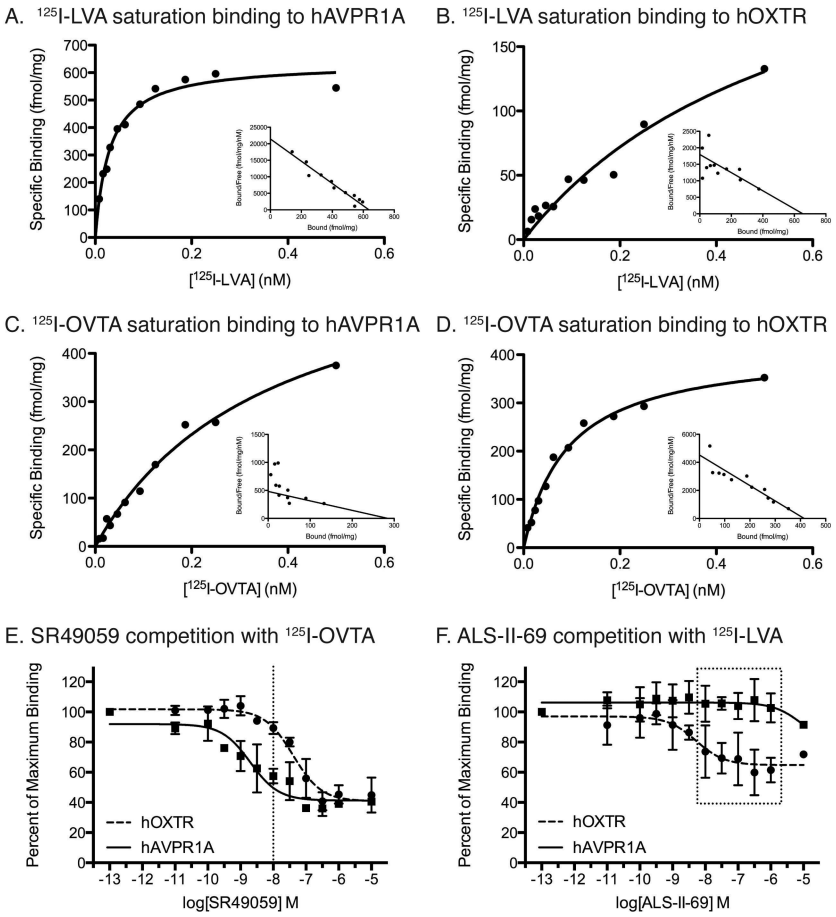

Figure 1. Pharmacology results from ligand binding assays

A-D. Saturation binding curves and scatchard plots (insets) for the AVPR1A and OXTR radioligands binding to hAVPR1A (A,C) and hOXTR (B,D). E,F. Competition binding curves for competitor ligands. E. Competition curves for the AVPR1A ligand SR49059 showing that 10^{-8} M, or 10 nM, is the optimal concentration to occupy hAVPR1A without binding significantly to hOXTR (dotted line). F. Competition curves for the OXTR ligand ALS-II-69 showing that this ligand does not begin to occupy hAVPR1A until 10^{-5} M, or 10 μM. Thus, this ligand can be used at concentrations ranging to 1 μM (dotted box).

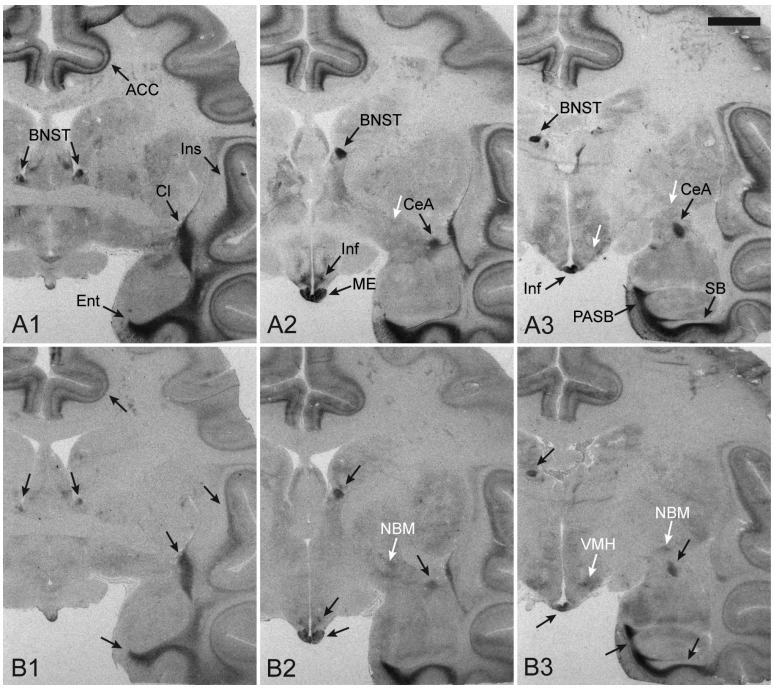

Figure 2. Radioligand binding to the rhesus macaque brain at three anatomical levels

The binding patterns produced by the AVPR1A radioligand, ^{125}I-LVA (A), and the OXTR radioligand, ^{125}I-OVTA (B), in rhesus monkey brain tissue sections at three anatomical levels (1, 2, 3), showing the overlap in binding by these two radioligands across brain regions. Black arrows indicate areas with overlapping binding between the two radioligands. White arrows highlight an example of two regions, the ventromedial hypothalamus and the nucleus basalis of Meynert, which has low levels of binding to ^{125}I-OVTA but not ^{125}I-LVA. Scale bar = 5mm. Abbreviations: ACC, anterior cingulate cortex; BNST, bed nucleus of stria terminalis; CeA, central amygdala; Cl, claustrum; Ent, entorhinal cortex; Inf, infundibulum; Ins, insular cortex; ME, median eminence; NBM, nucleus basalis of Meynert; PASB, parasubiculum; SB, subiculum; VMH, ventromedial hypothalamus

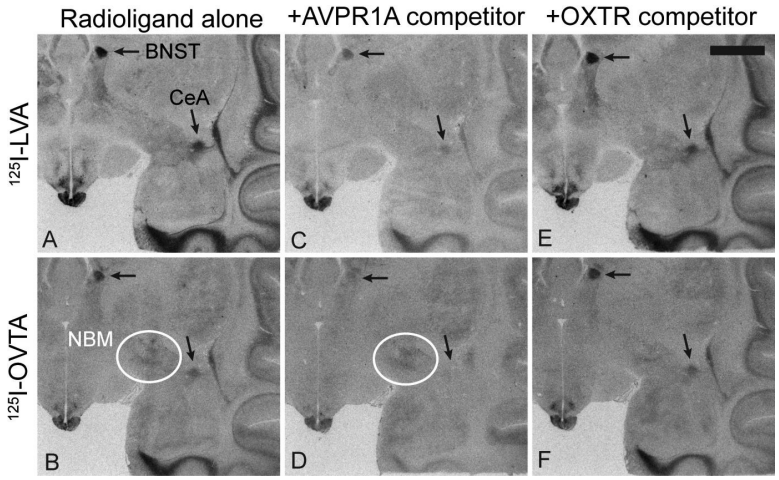

Figure 3. Representative results from competitive binding receptor autoradiography using ^{125}I-LVA and ^{125}I-OVTA

(A, B) Radioligand alone. (C, D) Radioligand coincubated with 10 nM of the AVPR1A competitor SR49059, showing that this compound is capable of competing off most of the signal from both radioligands, especially in the areas highlighted with arrows, the bed nucleus of stria terminalis (BNST) and the central amygdala (CeA). (E, F) Radioligand coincubated with 20 nM of the OXTR competitor ALS-II-69, showing little knockdown of ^{125}I-OVTA or ^{125}I-LVA compared to the radioligand alone condition. White circles in panels B and D indicate modest binding of ^{125}I-OVTA to the nucleus basalis of Meynert (NBM), an area which does not show binding to ^{125}I-LVA and does shows reduced binding in the presence of the OXTR competitor in panel F. Scale bar = 5mm.

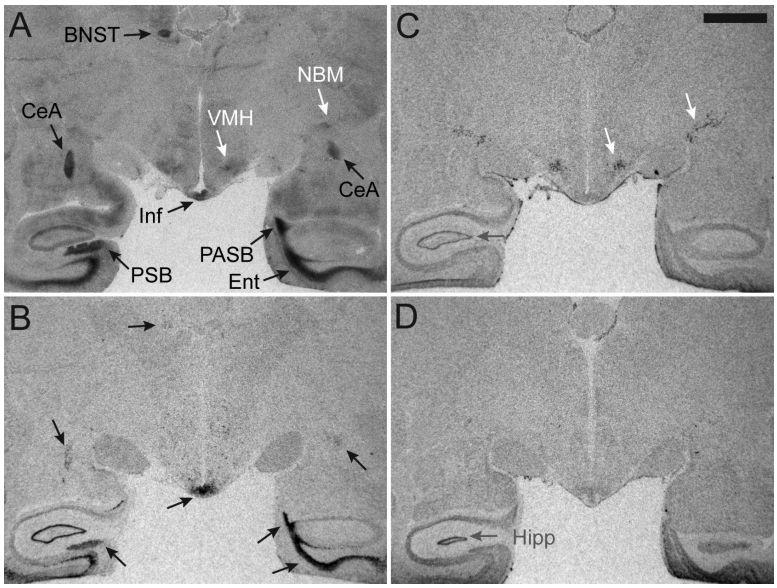

Figure 4. Comparison of ^{125}I-OVTA radioligand binding alone to *in situ* hybridization results

The binding pattern produced by ^{125}I-OVTA alone (A) includes binding to both AVPR1A and OXTR, which can be parsed apart by comparing the radioligand binding densities to the *in situ* hybridization results for mRNA for these receptors. (B) An antisense probe for AVPR1A mRNA yields a binding pattern that matches areas of radioligand binding (black arrows, A,B). (C) An antisense probe for OXTR mRNA yields a binding pattern which allows the remaining lighter gray densities produced by ^{125}I-OVTA to be interpreted as distinctly OXTR binding and not background (white arrows, A,C). (D) A sense probe designed as a negative control for *in situ* hybridization shows that the mRNA signal seen in the hippocampus and surrounding areas is background and not specific mRNA for OXTR (gray arrows, C,D). Scale bar = 5mm. Abbreviations: BNST, bed nucleus of stria terminalis; CeA, central amygdala; Ent, entorhinal cortex; Inf, infundibulum; NBM, nucleus basalis of Meynert; PASB, parasubiculum; PSB, presubiculum; VMH, ventromedial hypothalamus

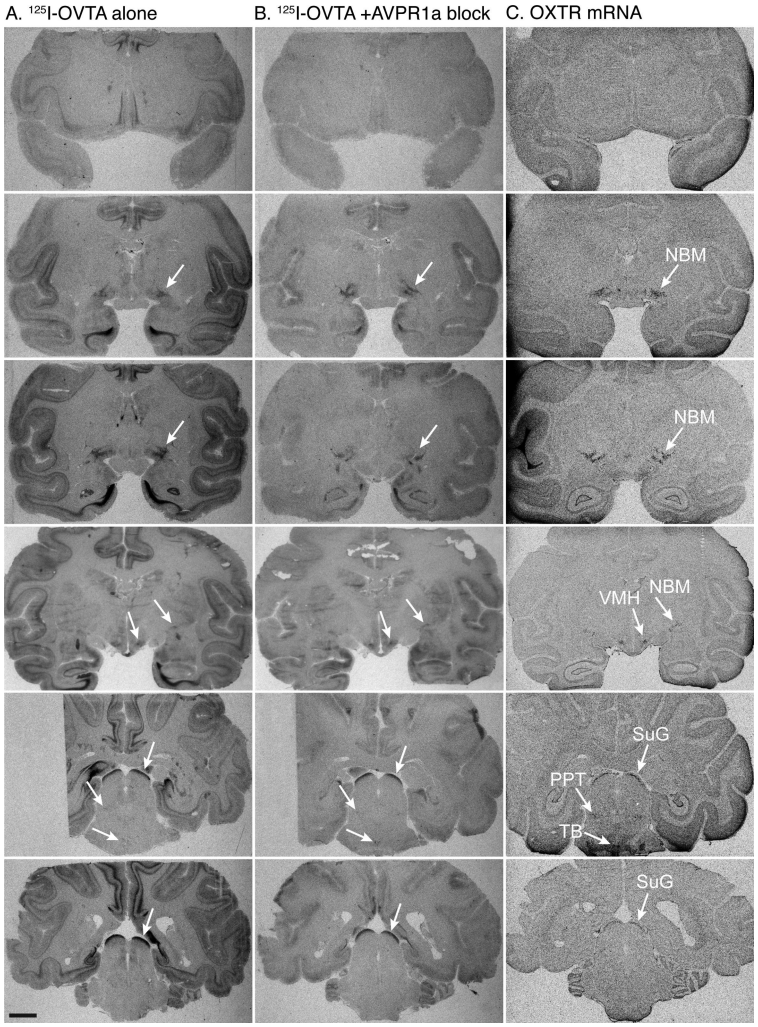

Figure 5. OXTR distribution in the rhesus macaque brain

Receptor autoradiography results using ^{125}I-OVTA alone (A) and ^{125}I-OVTA plus 10 nM SR49059 (B) aligned with *in situ* hybridization results for *OXTR* mRNA (C) in six representative individuals at six different levels (rows). White arrows indicate areas of specific OXTR expression based on a visual comparison of the results from *in situ* hybridization (C) and competitive binding (B). Scale bar = 5mm. Abbreviations: III, oculomotor nucleus; NBM, nucleus basalis of Meynert; PPT, pedunculopontine tegmental nucleus; SuG, superficial gray layer of the superior colliculus; TB, trapezoid body; VMH, ventromedial hypothalamus; Sp5, spinal trigeminal nucleus

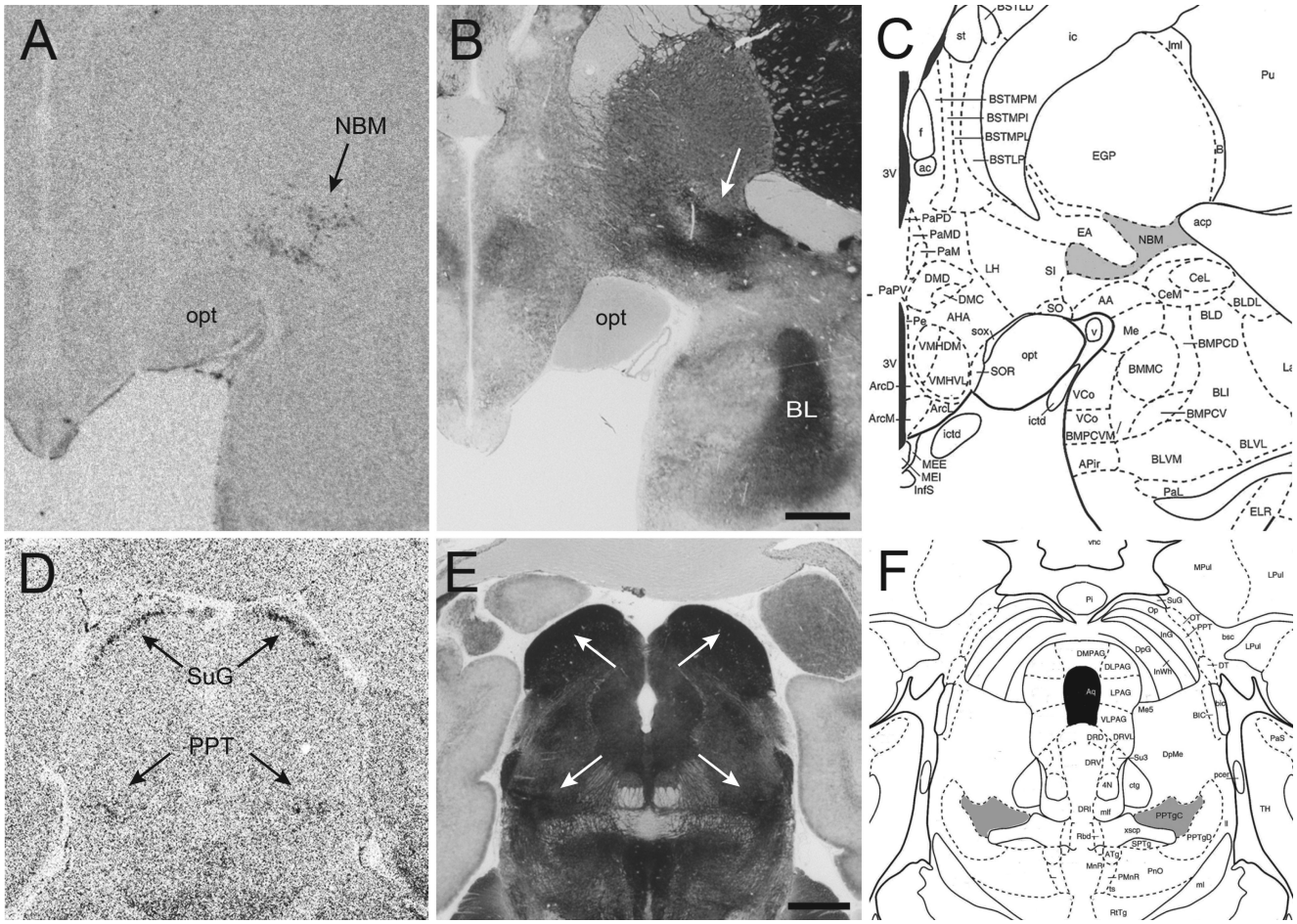

Figure 6. Comparison of OXTR mRNA distribution with acetylcholinesterase counterstained sections

Resulting OXTR mRNA at two anatomical levels (A, D) showing expression in the nucleus basalis of Meynert (NBM), the pedunculopontine tegmental nucleus (PPT), and the superficial gray layer of the superior colliculus (SuG). The adjacent acetylcholinesterase (AChE) counterstained sections (B, E) and adapted plates from the Paxinos rhesus brain atlas (C, F) show that OXTR expression is specific to the cholinergic NBM in the basal forebrain (gray area in panel C) and to the cholinergic subdivision of the PPT ("PPTgC", gray area in panel F). Scale bars = 2mm.